

Postnatal ontogenetic size and shape changes in the craniums of plateau pika and woolly hare (Mammalia: Lagomorpha)

Zhi-Gui ZHANG¹, De-Yan GE^{2,*}

1. Leshan Vocational and Technical College, Leshan, Sichuan 614099, China

2. Key Laboratory of Zoological Systematics and Evolution, Institute of Zoology, Chinese Academy of Sciences, Beijing 100101, China

Abstract: In the present study, postnatal ontogenetic size and shape changes in the cranium of two lagomorph species, the plateau pika (*Ochotona curzoniae*) and woolly hare (*Lepus oiostolus*), were investigated by geometric morphometrics. The ontogenetic size and shape changes of their cranium exhibited different growth patterns in response to similar environmental pressures on the Qinghai-Tibetan Plateau. The overall size change in the cranium of the plateau pika was slower than that of the woolly hare. The percentage of ontogenetic shape variance explained by size in the woolly hare was greater than that in the plateau pika. The overall shape of the cranium was narrowed in both species, and morphological components in relation to neural maturity showed negative allometry, while those responsible for muscular development showed isometric or positive allometry. The most remarkable shape variations in the plateau pika were associated with food acquisition (temporalis development), though other remarkable shape variations in the incisive and palatal foramen in the ventral view were also observed. The most important shape change in the woolly hare was demonstrated by the elongation of the nasal bones, expansion of the supra-orbital process and shape variation of the neurocranium.

Keywords: Ontogeny; Geometric morphometrics; Allometry; Cranial morphology; Lagomorpha

Leporidae, especially extant *Lepus* species, are among the most capable mammalian runners. They can jump significant distances (up to 6 meters), move in rapid zigzag patterns, and locomote bipedally if required. The craniums of leporids are characterized by fenestration on the side of the rostrum that extends to the posterior region of the skull, an anatomical feature believed to reduce skull mass (Bramble, 1989). The posterior cranium in hares also permits considerable intracranial movement, which may function as a shock-absorbing mechanism to minimize jarring during high-speed running (Bramble, 1989). However, the extant Ochotonidae species from the genus *Ochotona*, which are closely related sister taxa of Leporidae, show less ability in running. When encountering predators, they usually warn other individuals through highly specialized calls and rapidly seek shelter. The shape of the incisive and palatal foreman in *Ochotona* have been used as diagnostic characteristics in taxonomy (Lissovsky et al,

2008; Smith & Xie, 2009). The body size evolution of Leporidae and Ochotonidae demonstrates markedly different patterns, with extant species of the former group showing non-normal distribution, and extant species of the latter group showing significant normal distribution (Ge et al, 2013). However, why or how size changes in each group correspond to the overall shape variance of the cranium during postnatal development is unclear.

Of the known hares and pikas, the woolly hare (*L. Oiostolus*) and plateau pika (*O. curzoniae*) sympatrically inhabit a wide range of the Qinghai-Tibetan Plateau (QTP) and are both highly adapted to the cold and anoxic envir-

Received: 04 December 2013; Accepted: 14 April 2014

Foundation items: This project was partially supported by a grant (Y229YX5105) from the Key Laboratory of the Zoological Systematics and Evolution of the Chinese Academy of Sciences and the National Science Foundation of China (31101629)

*Corresponding author, E-mail: gedy@ioz.ac.cn

onment. Cranial growth patterns of these two species have not been studied, however, and it is unclear how different components of their cranium obtain their adult size and shape.

In the present study, we aimed to explore the size and shape changes in the cranium of the plateau pika and woolly hare through postnatal ontogeny, and discern the possible causes for the divergence in the growth rates of different morphological components. Geometric morphometrics were used to quantify and visualize the morphological variation in the dorsal, ventral and lateral cranium.

MATERIAL AND METHODS

Materials

A total of 84 cranium of *L. oiostolus* and 56 specimens of *O. curzoniae* were investigated. All cranium specimens were intact on at least one side of the cranium. The specimens represent the two species at different ages, and were mainly collected from the Qinghai-Tibet Plateau of China. All materials were preserved in the National Zoological Museum of China, Institute of Zoology, Chinese Academy of Sciences (IOZCAS) and the Northwest Institute of Plateau Biology, Chinese Academy of Sciences (NIPBCAS). Previous studies demonstrated insignificant sexual dimorphism in *Ochotona* and *Lepus*, which enabled the combination of males and females in all our analyses (Lu, 2003; Smith & Weston, 1990). Supplementary details on the specimens studied are given as Supplementary Table 1 (Supporting information of <http://www.zoores.ac.cn/>).

Photography

We viewed the dorsal, ventral and lateral cranium in this study. Photographs were taken using a Canon PowerShot S5IS (Japan) with a macro-focusing lens. To minimize measurement errors, all photos were taken by the corresponding author. For dorsal views, the camera was focused on the frontal region; for ventral views, the camera was focused on the tooth rows; and for lateral views, the camera was focused on the zygomatic arch. Images were standardized for skull position and camera lens plane as well as for distance between camera lens and the sample. All digital photos were taken with a scale bar parallel to the longitudinal axis of the cranium, which was set to record the size differences among specimens.

Data acquisition and partition

In total, 129 landmarks and semi-landmarks on the

right half of the skull in *O. curzoniae* were digitized for analysis, including 39 for the dorsal cranium, 55 for the ventral cranium, and 35 for the lateral cranium (Figure 1A1, A2 and A3). A total of 168 landmarks and semi-landmarks on the right half of the skull in *L. oiostolus* were digitized for analysis, which included 44 for the dorsal cranium, 62 for the ventral cranium, and 62 for the lateral cranium (Figures 1B1, B2 and B3). The locations of these landmarks and semi-landmarks mainly followed those of Ge et al (2012); detailed information is given in Table 1. Terminologies used in this study mainly followed Wible (2007). The landmarks and semi-landmarks were defined and digitized in tpsDig 2.0 (Rohlf, 2001) with MakeFan6 (Sheets, 2003), which offered identifiable and homologous locations on the skull. The scale factor was also generated in the data matrix with tpsDig, which set 1 cm of the scale bar recorded in the original images as 1. The raw datasets of each of the three views were examined in tpsSmall to test whether any specimens deviated largely from the whole dataset. Semi-landmarks were permitted to slide along the tangents to the curve to minimize bending energy between each specimen. The skulls of mammals can be divided into pre-orbital, inter-orbital and post-orbital regions (Lin & Shiraishi, 1992; Tanaka, 1942), which were extracted from the ventral view in the present study to respectively compare their ontogenetic size changes.

Morphometric analysis

Morphometric analysis of ontogenetic size and shape change in *O. curzoniae* and *L. oiostolus* was conducted using a generalized orthogonal least-squares Procrustes superimposition and relative warps analysis. Statistical analysis was based on centroid size, that is, the square root of the sum of squared distances of measured landmarks. Visualization of shape change was performed by thin-plate spline procedures. These analyses were conducted in the tps series of programs (Rohlf, 2001) and SPSS statistics 17.0 (SPSS inc., Chicago, IL, USA).

In the present study, centroid size was calculated from the ventral view of the whole cranium, and the pre-orbital, inter-orbital, and post-orbital regions in each of these two species. Growth rate (inferred from size change) of these regions was compared respectively. Centroid sizes of each of the three regions were regressed against the centroid size of the whole cranium to investigate the relative growth rate of each morphological partition. The null hypothesis was the size change of these small

partitions parallel to the size change of the whole cranium. The coordinate data of each view were regressed against centroid size in tpsRegr (Rohlf, 2001) to visualize the ontogenetic trajectories in different regions of the cranium by the direction and length of vectors. The Generalized Goodall F-test of significance (Goodall, 1991), with df_1 and df_2 degrees of freedom, was conducted. Shape changes from the smallest specimen to the largest specimen were illustrated by deformation grids.

RESULTS

Analyses in tpsSmall indicated that no specimen deviated from other specimens in each view for the two species (r ranged from 0.9999 to 1 for *L. oiostolus* and *O. curzoniae* in tpsSmall), which allowed us to use infant specimens in the present study. Geometric morphometric analyses demonstrated allometric growth in different cranium regions of the plateau pika and woolly hare. The cranium growth rates inferred from size change in the pro-orbital, inter-orbital, and post-orbital regions were higher in the woolly hare, though the growth of the pro-orbital region was nearly parallel in the two species. The inter-orbital

region in the plateau pika grew slightly slower than that in the woolly hare, while the post-orbital region of the woolly hare showed a no-linear growth pattern ($P=0.086$) (Figure 2).

Regressing size change on shape change demonstrated prominent allometry in the three views of the woolly hare (dorsal: $f=43.37$, $df=84$, 6384, $P<0.01$, size explained 36.03% of total shape variation; ventral: $f=26.2383$, $df=120$, 9840, $P<0.01$, size explained 24.13% of total shape variation; lateral: $f=26.87$, $df=120$, 8400, $P<0.01$, size explained 27.24% of total shape variation), and in the dorsal and ventral views of the plateau pika (dorsal: $f=10.82$, $df=74$, 3996, $P<0.01$, size explained 16.64% of total shape variation; ventral: $f=15.38$, $df=104$, 5512, $P<0.01$, size explained 22.43% of total shape variation), but a lower value was observed in the lateral view of the plateau pika ($f=0.25$, $df=66$, 3234, $P<0.01$, size explained 0.5% of total shape variation). These results indicated that the percentage of total ontogenetic shape variance explained by size in the woolly hare was higher than that in the plateau pika.

Plotting shape change vectors on consensus shape demonstrated that shape variation in the two species mainly occurred in the very early life stage (Figure 3).

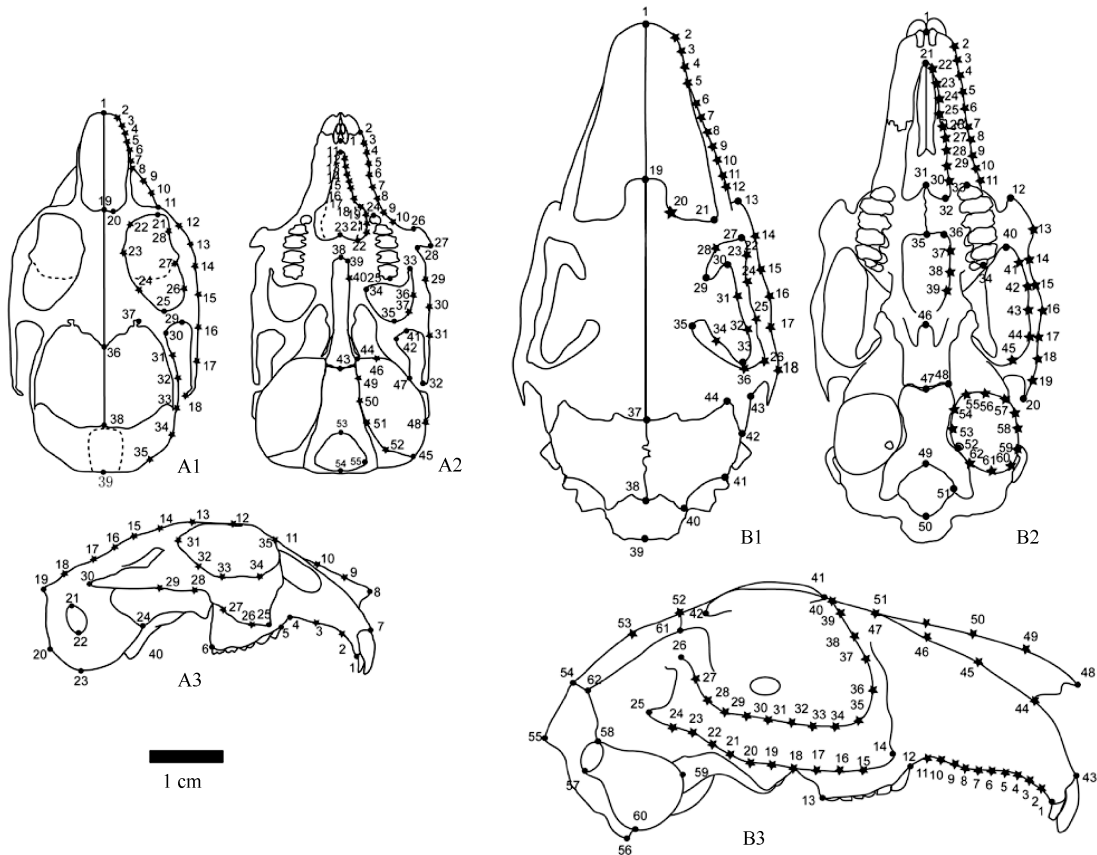


Figure 1 Landmark and semi-landmark locations

A1-A3: Dorsal, ventral and lateral views of *O. curzoniae*; B1-B3: Dorsal, ventral and lateral views of *L. oiostolus*.

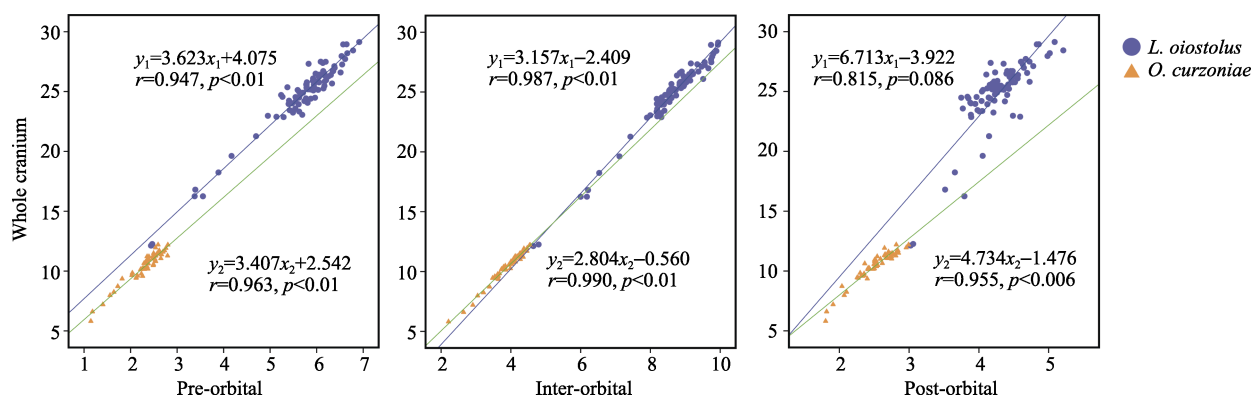


Figure 2 Size variation (centroid size) in the pre-orbital, inter-orbital and post-orbital regions of the cranium

Table 1 Definition of landmarks and semi-landmarks

<i>O. curzoniae</i>	<i>L. oiostolus</i>
Dorsal cranium	Dorsal cranium
1. Anterior tip of nasal bone	1. Anterior tip of nasal bone
2–10. Semi-landmarks along lateral margin of premaxilla and maxillary	2–12. Semi-landmarks along lateral margin of premaxilla and maxillary
11. Anterior tip of zygomatic in the lateral edge	13. Anterior tip of zygomatic in the lateral edge
12–17. Semi-landmarks along lateral edge of zygomatic arch and squamosal	14–18. Semi-landmarks along lateral edge of zygomatic
18. Most posterior end of zygomatic arch	19. Meeting point between nasal bone and frontal along longitudinal axial of cranium
19. Meeting point between nasal bone and frontal along longitudinal axial of cranium	20. Mid point between landmark 19 and 21
20. Posterior tip of nasal bone	21. Posterior tip of suture between nasal bone and frontal
21. Most anterior point of orbital	22–26. Semi-landmarks along interior edge of zygomatic
22. Mid point between 21 and 23	27. Anterior meeting point between zygomatic and frontal
23. Most internal point of orbital	28. Mid point between 27 and 29
24. Mid point between 23 and 25	29. Most posterior beginning of anterior supraorbital process
25. Most posterior point of orbital	30. Anterior tip of anterior supraorbital process
26–28. Semi-landmarks along internal edge of zygomatic arch	31–32. Semi-landmarks between landmark 30 and 33
29. Posterior point of the zygomatic process of squamosal body	33. Posterior tip of posterior supraorbital process
30. Posterior point at the joining of squamosal body to the zygomatic process of squamosal	34. Most anterior beginning of posterior supraorbital process
31–35. Semi-landmarks along posterior edge of cranium	35–36. Semi-landmarks along posterior contour of orbital
36. Meeting point of frontal and parietal along longitudinal axial of cranium	37. Meeting point of frontal and parietal along longitudinal axial of cranium
37. Most anterior meeting point of frontal and parietal	38. Meeting point of parietal and supraoccipital along longitudinal axial of cranium
38. Meeting point of parietal and supraoccipital along longitudinal axial of cranium	39. Most posterior point of the supraoccipital along longitudinal axial of cranium
39. Most posterior point of the supraoccipital along longitudinal axial of cranium	40. Most posterior point of parietal
Ventral cranium	41. Most anterior meeting point of parietal and supraoccipital
1. Meeting point of incisors	42. Most lateral point of parietal
2. Most posterior end of incisors along lateral edge	43. Semi-landmarks along lateral margin of squamosal
3–10. Semi-landmarks along lateral edge of premaxilla and maxillary	44. Most anterior point of parietal meeting with frontal and squamosal
11. Most anterior edge of incisive and palatal foramen	Ventral cranium
12–21. Semi-landmarks along incisive and palatal foramen	1. Meeting point of incisors
22. Most posterior end of the incisive and palatal foramen	2–11. Semilandmarks along lateral edge of premaxilla and maxillary
23. Posterior end of the incisive and palatal foramen along longitudinal axial of the cranium	12. Most anterior point of zygomatic
24. Anterior end of tooth row	13–20. Semi-landmarks along lateral edge of zygomatic
25. Posterior end of tooth row	21–30. Semi-landmarks along internal edge of premaxilla and maxillary
26. Most anterior end of masseteric spine	31. Anterior end of the incisive and palatal foramen along longitudinal axial of cranium
27. Apex of masseteric spine	32. Posterior end of the incisive and palatal foramen
28. Most posterior end of masseteric spine	33. Anterior end of the cheek tooth row
29–31. Semi-landmarks along lateral edge of zygomatic arch and the zygomatic process of squamosal	34. Posterior end of the cheek tooth row
32. Most posterior end of the zygomatic process of squamosal	35. Posterior end of palatal bridge along longitudinal axial of cranium
33. Most anterior end of orbital	36. Anterior end of palatal bridge
34. Most internal end of orbital	37–39. Semi-landmarks along lateral margin of entopterygoid crest
35. Most posterior end of orbital	40. Most anterior end of orbital
36–37. Semi-landmarks along lateral edge of orbital	41–45. Semi-landmarks along internal edge of zygomatic
38. Posterior end of palatine along longitudinal axis	46. Anterior end of basisphenoid along longitudinal axial of cranium
39–40. Semi-landmarks along entopterygoid crest	47. Most anterior point of basisphenoid meeting with basisphenoid
41. Posterior point of zygomatic process of squamosal body	48. Lateral end of basisphenoid meeting with basisphenoid
42. Contact point of glenoid fossa with alisphenoid	49. Most anterior end of foreman magnum
43. Mid point of basioccipital	
44. Anterior point of tympanic bulla	
45. Posterior point of tympanic bulla	
46–48. Semi-landmarks along lateral edge of tympanic bulla	
49–52. Semi-landmarks along internal edge of tympanic bulla	

(Continued)

<i>O. curzoniae</i>	<i>L. oiostolus</i>
53. Most anterior point of foramen magnum 54. Most posterior end of foramen magnum 55. Most lateral point of foramen magnum	50. Most posterior end of foramen magnum 51. Most lateral end of foramen magnum 52. Opening of external carotid artery 53–62. Semi-landmarks along tympanic bulla
Lateral cranium	Lateral cranium
1. Center of alveolar ridge over maxillary incisor 2–3. Semi-landmarks along lower edge of premaxilla and maxillary 4. Most upper point of maxillary 5. Most anterior end of tooth row 6. Most posterior end of tooth row 7. Most anterior end of cheek tooth 8. Most anterior end of nasal bone 9–18. Semi-landmarks along upper ridge of the cranium 19. Posterior end of the cranium 20. Most upper point of tympanic bulla opening 21. Most lower point of tympanic bulla opening 22. Most basal point of basioccipital 23. Most lower end of tympanic bulla 24. Most internal end of tympanic bulla 25. Most lateral end of zygomatic arch 26–29. Semi-landmarks along lateral edge of zygomatic arch 30. Most posterior end of orbital 31–35. Semi-landmarks along upper edge of zygomatic arch	1. Center of alveolar ridge over maxillary incisor 2–11. Semi-landmarks along lower edge of premaxilla and maxillary 12. Anterior end of cheek tooth raw 13. Posterior end of cheek tooth raw 14. Most anterior point of zygomatic 15–24. Semi-landmarks along lower edge of zygomatic 25. Most posterior end of zygomatic 26. Most posterior end of orbital 27–40. Semi-landmarks along orbital 41. Anterior end of supraorbital process 42. Posterior end of supraorbital process 43. Anterior end of incisive 44–47. Semi-landmarks along upper edge of premaxilla and maxillary 48. Anterior end of nasal bone 49–51. Semi-landmarks along upper edge of nasal bone 52–53. Semi-landmarks along posterior cranium 54. Most superior end of occipital 55. Posterior end of occipital 56. Most lower end of paroccipital process 57. Most lower point of tympanic bulla opening 58. Most upper point of tympanic bulla 59. Most anterior point of tympanic bulla 60. Most lower point of tympanic bulla 61. Meeting point of frontal, parietal and sphenoid bones 62. Meeting point of supraoccipital, parietal and sphenoid bones

Details are also shown in Figure 1.

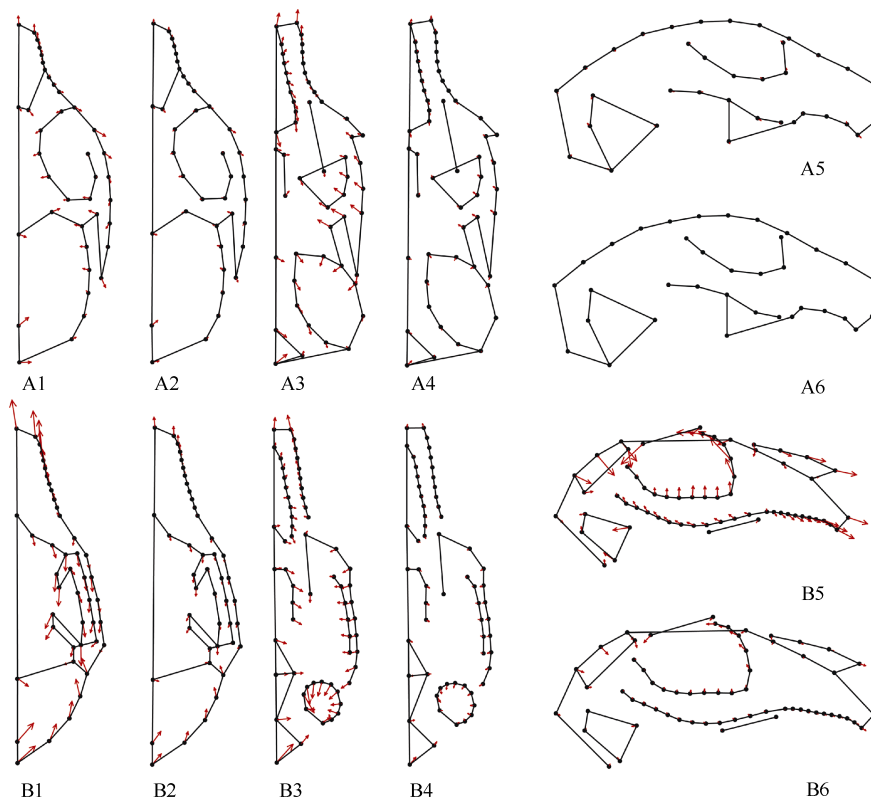


Figure 3 Growth trajectories in different views of the cranium

A1–A6: *O. curzoniae*, A1–A2, dorsal view; A3–A4, ventral view; A5–A6, lateral view. B1–B6: *L. oiostolus*, B1–B2, dorsal view; B3–B4, ventral view; B5–B6, lateral view. 1, 3, 5 of AB show variation in the early life stage; 2, 4, 6 show variation at near adulthood.

The overall shape of the plateau pika was narrowed, and the anterior ridge of the zygomatic arch was expanded slightly. Incisive and palatal foreman showed prominent shape variation from infants to adults. The lateral view of the cranium showed less shape variation compared with the other two views. The woolly hare exhibited a wider range of shape variation than that of the plateau pika, and the general shape of its cranium was also narrowed with a remarkable shape change in the nasal bone region and contraction of the tympanic bulla. The super-orbital process displayed prominent enlargement in both the anterior and posterior branches. The relative size of the neurocranium was reduced, the relative size of the tympanic bulla was greatly reduced and the incisive and palatal foramen showed less variation. For plateau pika, regressing centroid size on shape variables also indicated that small morphological components in the pre-orbital region (in all three views) was dominated by positive allometry, while those in the inter-orbital and post-orbital regions (dorsal and ventral views) showed prominent negative allometry. In the woolly hare, however, morphological

components in the pro-orbital and inter-orbital regions were mainly dominated by isometry and positive allometry, while a prominent negative allometry was observed in the post-orbital region. A detailed comparison of the shape variation in small morphological components between the two species is given in Figure 4.

DISCUSSION

In light of the highly specialized skull morphology and rapid skull development in the plateau pika and woolly hare, as well as their short period of offspring dependence, the special growth patterns of their craniums are likely the result of combined pressure for food acquisition and other strategies for survival. Natural selection may favor the rapid development of adult morphology to improve food acquisition, locomotion performance, and predator avoidance. The occurrence of different growth rates in specific morphological components suggests selective pressures on different parts of the cranium during postnatal growth.

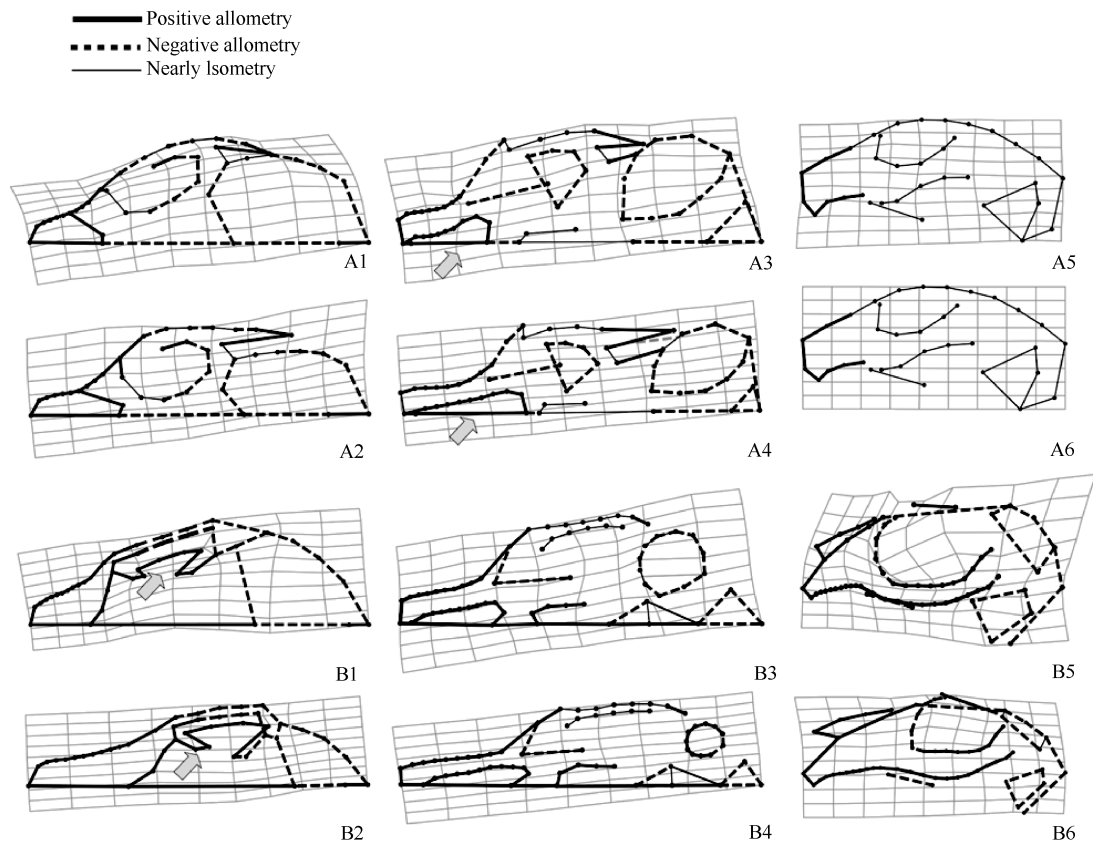


Figure 4 Shape variation from the smallest to largest specimens

A1–A6: *O. curzoniae*, A1–A2, dorsal view; A3–A4, ventral view; A5–A6, lateral view. B1–B6: *L. oiostolus*, B1–B2, dorsal view; B3–B4, ventral view; B5–B6, lateral view. Arrows indicate prominent shape variation in incisive and palatal foreman of *O. curzoniae* and supra-orbital process of *L. oiostolus*.

Acknowledgements: We thank Prof. Fu-Ming LEI and the anonymous editors and reviewers for their constructive suggestions in improving this manuscript. We would also

like to thank Dr. Wen-Jing LI and Mrs. Xiao-Ping CAO for their assistance when studying specimens under their curation.

References

- Bramble DM. 1989. Cranial specialization and locomotor habit in the lagomorpha. *American Zoologist*, **29**(1): 303-317.
- Ge DY, Lv XF, Xia L, Huang CM, Yang QS. 2012. Geometric morphometrics of postnatal size and shape changes in the cranium of cape hare (Lagomorpha, Leporidae, *Lepus capensis*). *Acta Theriologica Sinica*, **32**(1): 12-24.
- Ge DY, Wen ZX, Xia L, Zhang ZQ, Erbajeva M, Huang CM, Yang QS. 2013. Evolutionary History of Lagomorphs in Response to Global Environmental Change. *PLoS ONE*, **8**(4): e59668.
- Goodall C. 1991. Procrustes Methods in the Statistical-Analysis of Shape. *Journal of the Royal Statistical Society Series B-Methodological*, **53**(2): 285-339.
- Lin LK, Shiraishi S. 1992. Skull growth and variation in the Formosan wood mouse, *Apodemus semotus*. *Journal of the Faculty of Agriculture Kyushu University*, **37**(1): 51-69.
- Lissovsky AA, Yang Q, Pilnikov AE. 2008. Taxonomy and distribution of the pikas (*Ochotona*, Lagomorpha) of alpina-hyperborea group in North-East China and adjacent territories. *Russian Journal of Theriology*, **7**(1): 5-16.
- Lu X. 2003. Postnatal growth of skull linear measurements of Cape hare *Lepus capensis* in northern China: An analysis in an adaptive context. *Biological Journal of the Linnean Society*, **78**(3): 343-353.
- Wible JR. 2007. On the cranial osteology of the Lagomorpha. *Bulletin of Carnegie Museum of Natural History*, **39**(5): 213-234.
- Rohlf FJ. 2002. TPS series. Department of Ecology and Evolution, State University of Newyork, Stony Brook, New York. <http://life.bio.sunysb.edu/morph/>.
- Sheets HD. 2003. IMP-Integrated Morphometrics Package. Department of Physics, Canisius College, Buffalo, New York. <http://www.canisius.edu/~sheets/morphsoft.html>.
- Smith AT, Weston ML. 1990. *Ochotona princeps*. *Mammalian Species*, **352**: 1-8.
- Smith AT, Xie Y. 2009. *A Guide to the Mammals of China*. Princeton & Oxford: Princeton University Press. 1-544.
- Tanaka R. 1942. A biostatistical analysis of *Apodemus agmrius* from Formosa with special reference to its systematic characters. *Memoirs of the Faculty of Science and Agriculture, Taihoku Imperial University / Taihoku*, **23**, 212-285.